

## A multi level space phasor based PWM strategy for an open – end winding induction motor drive using two inverters with different DC link voltages

E.G Shivakumar, V.T Somasekhar, Krushna K. Mohapatra, K.Gopakumar, SM IEEE,  
L.Umanand, S.K Sinha.

**Abstract:** An open-end winding induction motor drive fed from two inverters with different DC link voltages is proposed in this paper. A total of 64 voltage space phasor combinations are possible in this scheme as each inverter produces 8 voltage space phasors. The proposed scheme produces voltage space phasor locations more than that of a 3-level inverter. A total of 37 space phasor locations are possible from the proposed scheme as compared to 18 voltage space phasor locations in a 3-level inverter. In the proposed scheme the induction motor neutral connection is separated (open- end winding) and fed from both the ends. Two 2-level inverters with DC link voltages of  $2/3$  Vdc and  $1/3$  Vdc are used for driving the motor. Here Vdc is the conventional 2-level inverter DC link voltage for identical power. A combination of two 2-level inverters with  $2/3$  Vdc and  $1/3$  Vdc DC-link voltages will produce a total of 64 voltage space phasor combinations in 37 space phasor locations. For the present scheme a space phasor based PWM scheme will produce stepped voltage waveforms for the motor phases in different speed ranges. The whole voltage space phasor locations can be divided into three regions according to the speed range. In the lower speed range the PWM phase voltage will have a six-step envelope (similar to the conventional scheme) and in the middle range the PWM motor phase voltage will have an 12-step envelope and the outer speed range (including the over modulation) the PWM motor phase voltage will have an 18- step envelope. A simple and elegant space phasor based PWM scheme is proposed in all sectors based on three phase motor reference voltages only. The sector identification is achieved by comparing the components of the motor reference voltages, using simple hysteresis comparators, along the three orthogonal axes to the a,b,c phase axes. The whole scheme is studied for a 1HP open- end winding motor and the results of the study including the over modulation ranges are presented in this paper.

**Index Terms**— Multi level inverters, PWM techniques, Induction motor drives.

E.G Shiva kumar, V.T Somasekhar, and Krushna Keshav Mohapatra are research students at CEDT, Indian Institute of Science, Bangalore, INDIA-560012.

K.Gopakumar is with CEDT, Indian Institute of Science, Bangalore-560012, INDIA(e-mail:kgopa@cedt.iisc.ernet.in)

L.Umanand and S.K. Sinha are with CEDT, IISc, Bangalore-560012, INDIA

### I. Introduction

The schematic of the dual voltage source inverter fed three-phase induction motor with open-end winding is shown in Fig. 1.  $V_{a0}$ ,  $V_{b0}$ ,  $V_{c0}$  are the pole voltages of the inverter-1.  $V_{a'o}$ ,  $V_{b'o}$ ,  $V_{c'o}$  are the pole voltages of inverter-2. The space phasor locations from individual inverters are also shown in Fig.2. Inverter-1 and Inverter-2 are fed from two isolated supply voltages of  $2/3$  Vdc and  $1/3$  Vdc each. A controlled DC link supply (Regenerative or with dynamic braking) is needed for the present scheme, otherwise the high voltage converter ( $2/3$  Vdc) can over charge the DC link capacitor of the lower converter in some space phasor combinations in PWM operation (11', 22' 33' 16', 15' etc);[3]. Here Vdc is the equivalent conventional 2-level inverter DC link voltage, The space phasor combinations (64- combinations) from the two inverters are shown in Fig.3. The combined 64 voltage space phasors are placed in 37 locations formed by equilateral triangles of sides  $1/3V_{dc}$  ( Fig.2). There are a total of 54 equilateral triangular sectors with  $1/3V_{dc}$  is possible with the proposed scheme as compared 6-triangular sectors of sides Vdc in a conventional one 2-level inverter drive. A voltage space phasor based PWM scheme for the present scheme is proposed in this paper. The 54 triangular sectors can be grouped into three sections for the PWM strategy depending on the modulation index for a V/f drive. For lower speed operation the PWM is confined to the inner hexagon formed by the triangular sectors 1 to 6 (Fig.2). In the middle speed range the PWM is confined in the middle triangular sectors formed by sectors 7 to24 (Fig.2). For the outer speed range the PWM is confined within the outer triangular sectors formed by 25 to 54. In the present scheme stepped PWM motor phase voltage will have an envelope of six-step in the lower speed range and an envelope of twelve-step in the middle sectors, In outer sectors, the motor PWM phase voltage will have eighteen-steps in a cycle of operation. As the number of steps increases the motor phase voltage will be smooth with lesser harmonic content as compared to a conventional drive, for the same PWM switching frequency. A simple space phasor based PWM scheme is presented in the following sections for all the sectors. The proposed PWM scheme in a sector is based only on the instantaneous magnitude of motor reference phase voltages[4].

### 11. Space phasor based PWM switching strategy for inner sectors:

If the tip of the reference voltage space-phasor lies in the inner hexagon (sectors1 to 6) with center at O (Fig.2), a space phasor based scheme as suggested in reference [4]

has been adopted. In this scheme [4], a space phasor based **PWM** strategy is proposed based on the instantaneous values of the reference voltages of a, b, c phases. This method does not depend on the magnitude of the reference voltage space phasor and its relative angle with respect to the reference axis ( $\alpha$  - axis placed along 'a' phase axis). The imaginary switching times for each phase which are proportional to the instantaneous phase voltage reference magnitudes  $v_a^*$ ,  $v_b^*$  and  $v_c^*$  are defined as follow [4]:

$$\begin{aligned} T_{as} &\equiv (T_s/V'_{dc}) v_a^* ; T_{bs} \equiv (T_s/V'_{dc}) v_b^* ; \\ T_{cs} &\equiv (T_s/V'_{dc}) v_c^* \end{aligned} \quad (1)$$

where  $T_s$  is the sampling time period for the **implementation** of the voltage space phasor modulation and  $v_a^*$ ,  $v_b^*$ ,  $v_c^*$  are the instantaneous values of the reference voltages of a, b, c phases and  $V'_{dc}$  is the amplitude of the triangular sectors ( $V'_{dc} = 1/3 V_{dc}$ ). The effective time-  $T_{eff}$  has been defined as the difference between the maximum and minimum values among  $T_{as}$ ,  $T_{bs}$  and  $T_{cs}$  and is the time duration for which the effective voltage is supplied to the load during a sampling period  $T_s$ . The time duration  $T_0$ , the time for which a zero vector (zero vectors are for inner sectors only) is applied, may be obtained from  $T_1$  and  $T_2$  as [4]:

$$T_0 = (T_s - T_{eff}) \quad (2)$$

$$\begin{aligned} \text{where } T_{eff} &= \max\{T_{as}, T_{bs}, T_{cs}\} - \min\{T_{as}, T_{bs}, T_{cs}\} \\ &= T_{max} - T_{min} \end{aligned} \quad (3)$$

The offset time  $T_{offset}$  required to distribute the zero voltage symmetrically during one sampling period is given by [4] :

$$T_{offset} = (T_0/2) - T_{min} \quad (4)$$

The actual switching times for each the inverter leg can be obtained by the time shifting operation as follows:

$$\begin{aligned} T_{ga} &= T_{as} + T_{offset} ; T_{gb} = T_{bs} + T_{offset} ; \\ T_{gc} &= T_{cs} + T_{offset} \end{aligned} \quad (5)$$

This method is extended for the proposed dual inverter scheme ( for **PWM** pattern generation in inner sectors '1' through '6') by clamping an inverter-1 at one end of the load phase (switching vector is either 7 or 8) while the inverter-2 at the other end is switched. The actual switching times for inverte-2 in inner sector is obtained in the same way as that of the single inverter scheme [4]. Each cycle of the load phase voltage is divided into 48 equal sub-intervals and the reference phase voltages are sampled 48 times in a cycle of operation. Each of this sub-interval duration corresponds to the sampling interval,  $T_s$ . This division is maintained for the entire modulation range with  $V/f$  control.

$$\begin{aligned} 0 \leq V_{ja}^* < V_{dc} \cos 30^\circ, 0 > V_{jb}^* \geq -\frac{V_{dc}}{3} \cos 30^\circ, \\ 0 < V_{jc}^* < \frac{V_{dc}}{3} \cos 30^\circ \end{aligned} \quad (6)$$

where  $V_{ja}^*$ ,  $V_{jb}^*$ ,  $V_{jc}^*$  are the orthogonal components of the reference phase voltages

### III. Space Phasor Based **PWM** switching signal generation for middle and outer sectors

Fig.2 Shows space phasor locations from the proposed dual inverter scheme. The space phasor combinations from the individual inverters are located at the vertices of various triangular sectors ( 54- triangular sectors) with amplitudes of the sides equal to  $1/3 V_{dc}$ . The inner triangular sectors can be grouped into a hexagon( similar to the conventional 2-level single inverter space phasor combinations)[4]. All the other outer triangular sectors can also be grouped into various hexagonal structure with centers at A to G as shown in Fig.2 [7]. If the center 'G' of the hexagonal structure formed by sectors 7,24,53, 54,25 and 26 is shifted to center 'O', the sector- 7 will be mapped to the inner sector-3, sector-24 will be mapped to sector-4, sector-53 will be mapped to sector-5 etc.. This implies that once the hexagonal center 'G' is shifted to inner hexagonal center 'O', the switching times  $T_{ga}$ ,  $T_{gb}$  and  $T_{gc}$  (eqn.5) for the inner sectors and the corresponding mapped sectors are identical [4] [7]. Only the inverter switching vectors are different based on the sector formation [ 7]. Similar way all the outer sectors can be mapped to the inner sectors using appropriate outer hexagonal centres, and the switching times  $T_{ga}$ ,  $T_{gb}$  and  $T_{gc}$  for all the outer triangular sectors can be calculated. Once the switching times are calculated the inverter switching vector sequences are selected based on the sector identification [7]. This will result in a very efficient way of computing switching times for all the outer sectors without much computation. A detailed explanation of this will be provided in the final version of the paper.

#### 3a. Sector identification

The sector identification is based on simple comparators along the axes orthogonal ( $ja, jb, jc$ ) to  $a, b, c$  axes. The lines  $f_i, e_j, dk, cT, bU, aV$ , and  $ZW$  are perpendicular the  $ja$  axis orthogonal to phase -  $a$  axis with voltage level from  $-V_{dc} \cos 30^\circ$  to  $V_{dc} \cos 30^\circ$  in steps of  $(v_{dc}/3) \cos 30^\circ$ . In a similar way the comparator levels along the  $jb$  and  $jc$  axes are also divided the same way as in  $ja$  axis. For example sector -1 identification can be done based on following equation.

Once the sector identification is completed the required outer sector can be mapped to the inner sector. Now shifting the point 'A' to the origin implies mapping the hexagon around 'A' to the inner hexagon with centre 'O'. If  $V_a, V_b, V_c$  are the motor reference phase

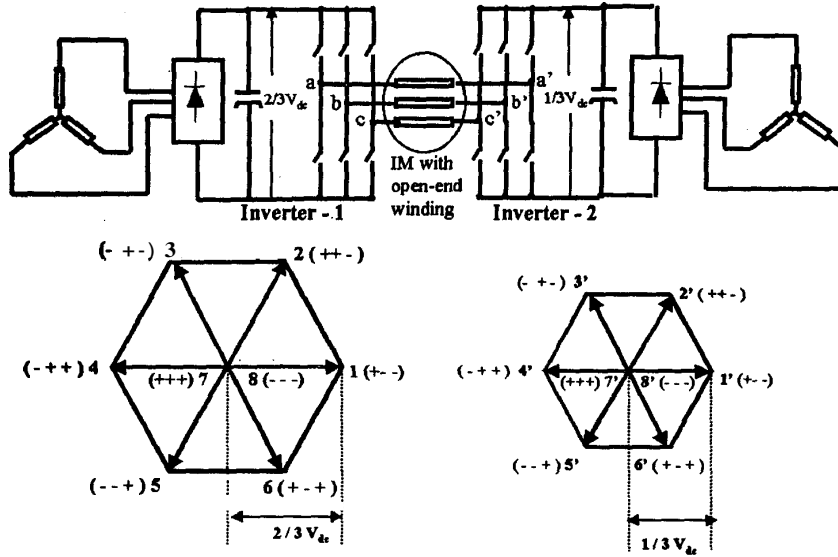


Fig.1 Dual-inverter fed induction motor with open-end winding with unequal voltages showing individual space-phasor locations

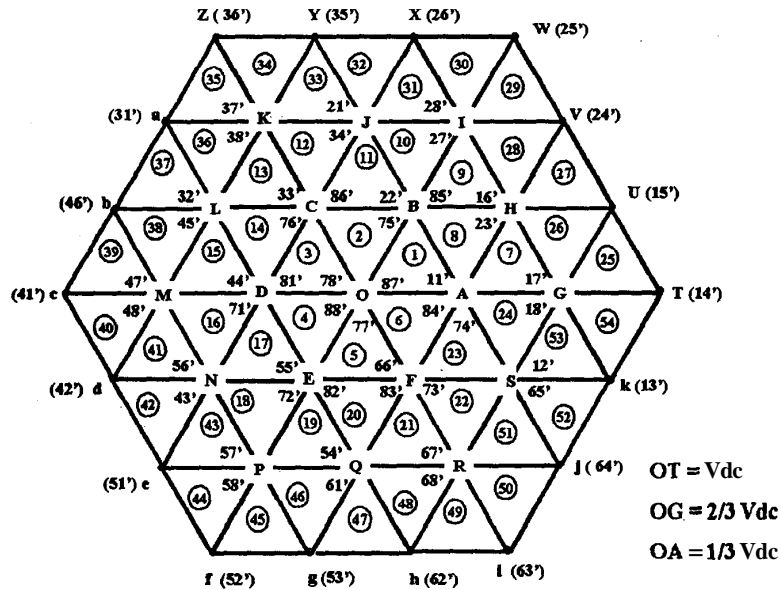


Fig.2 Space-phasor combinations for asymmetrical voltage dual-inverter drive

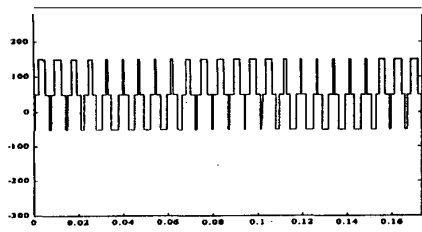


Fig.3a Phase voltage,  $|V_{s1}| = 0.2V_{dc}$

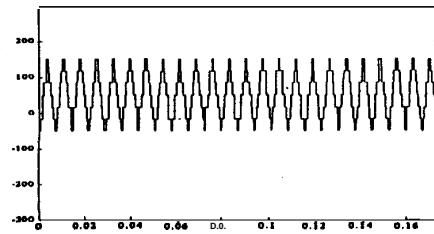


Fig.3b Triplen harmonic content,  $|V_{s1}| = 0.2V_{dc}$

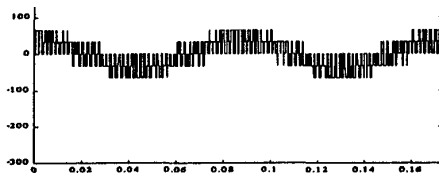


Fig.3c Actual motor phase voltage,  $|V_{s1}| = 0.2V_{dc}$

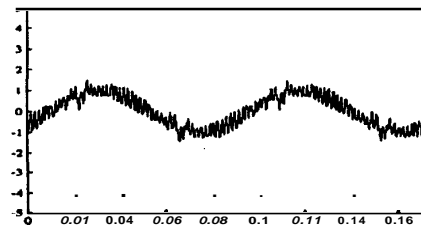


Fig.3d Motor phase current,  $|V_{s1}| = 0.2V_{dc}$

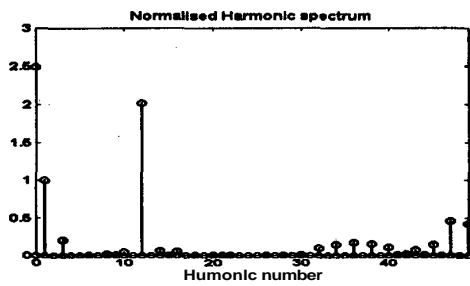


Fig.3e Harmonic spectrum of the phase voltage with the triplen content,  $|V_{s1}| = 0.2V_{dc}$

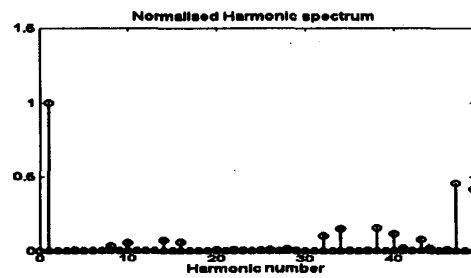


Fig.3f Harmonic spectrum of actual phase voltage,  $|V_{s1}| = 0.2V_{dc}$

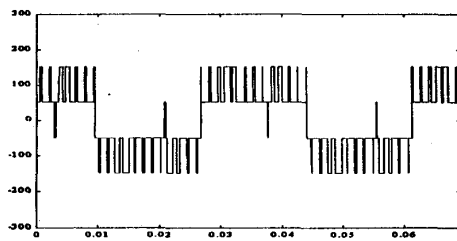


Fig.4a Phase voltage,  $|V_{s1}| = 0.5V_{dc}$

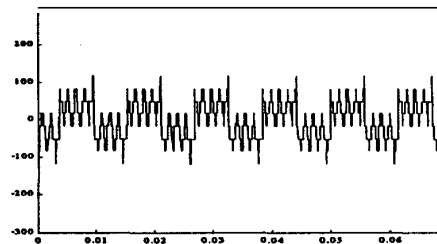


Fig.4b Triplen harmonic content,  $|V_{s1}| = 0.5V_{dc}$

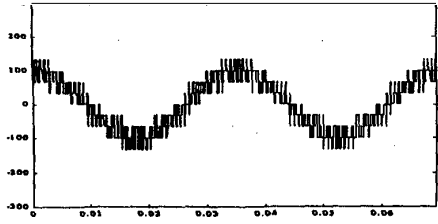


Fig.4c Actual motor phase voltage,  $|V_{ref}| = 0.5V_{dc}$

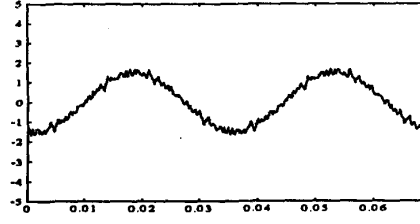


Fig.4d Motor phase current,  $|V_{ref}| = 0.5V_{dc}$

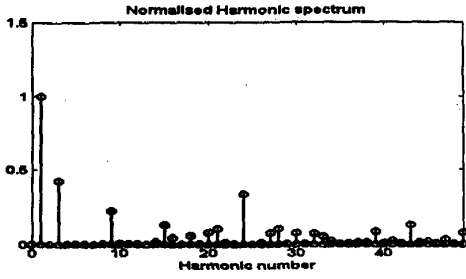


Fig.4e Harmonic spectrum of the phase voltage with the triplen harmonic content,  $|V_{ref}| = 0.5V_{dc}$

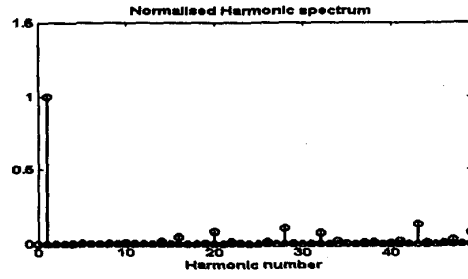


Fig.4f Harmonic spectrum of actual phase voltage

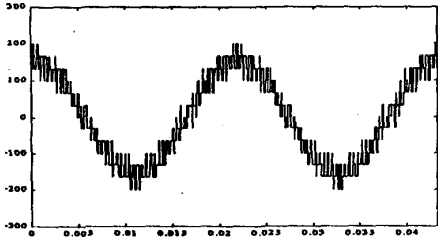


Fig.5a Actual motor phase voltage,  $|V_{ref}| = 0.8V_{dc}$

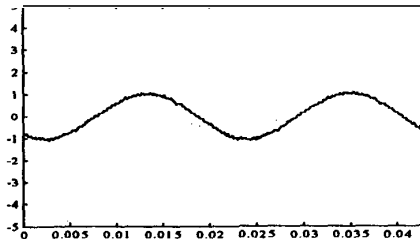


Fig.5b Motor phase current,  $|V_{ref}| = 0.8V_{dc}$

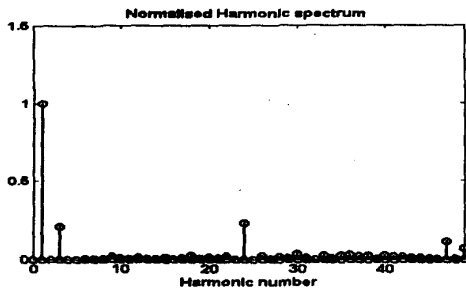


Fig.5c Harmonic spectrum of the phase voltage with the triplen content,  $|V_{ref}| = 0.8V_{dc}$

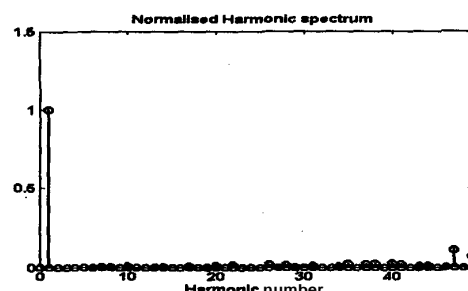


Fig.5d Harmonic spectrum of actual phase voltage,  $|V_{ref}| = 0.8V_{dc}$

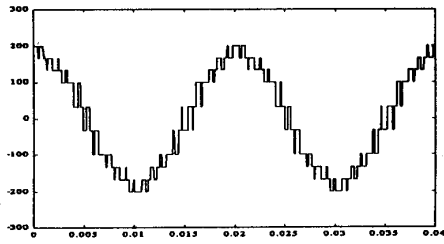


Fig.6a Actual motor phase voltage,  $|V_m| = V_{dc}$  (over-modulation)

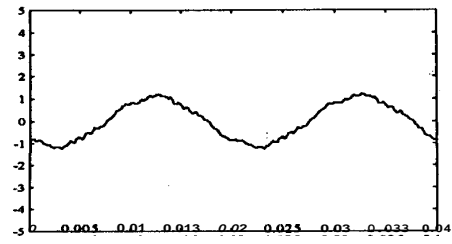


Fig.6b Actual motor phase voltage,  $|V_m| = V_{dc}$  (over-modulation)

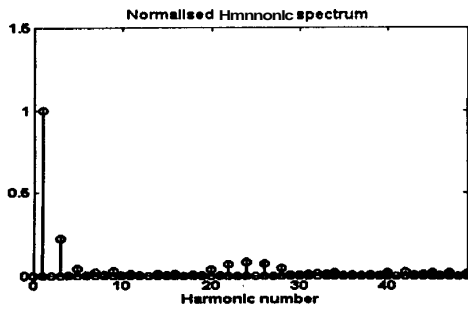


Fig.6c Harmonic spectrum of the phase voltage with the triplen harmonic content,  $|V_m| = V_{dc}$  (Over-modulation)

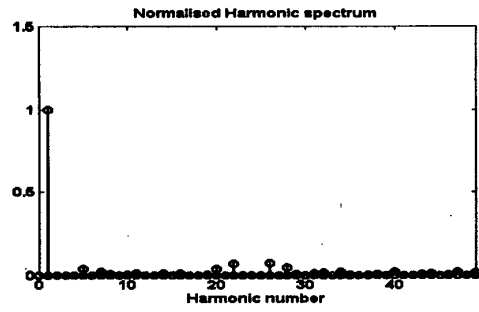


Fig.6d Harmonic spectrum of the actual phase voltage  $|V_m| = V_{dc}$  (Over-modulation)

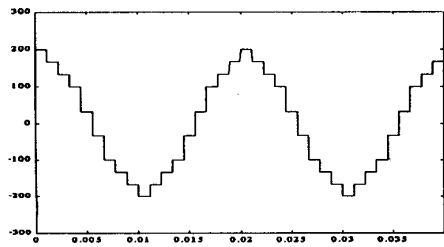


Fig.7a Actual motor phase voltage (18-step operation)

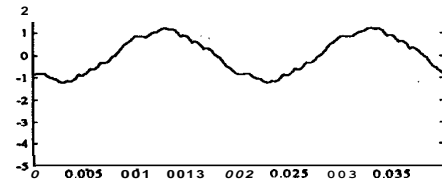


Fig.7b Motor phase current (18-step operation)

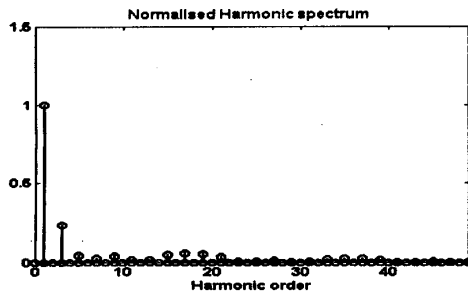


Fig.7c Harmonic spectrum of the phase voltage with the triplen harmonic content (18-step operation)

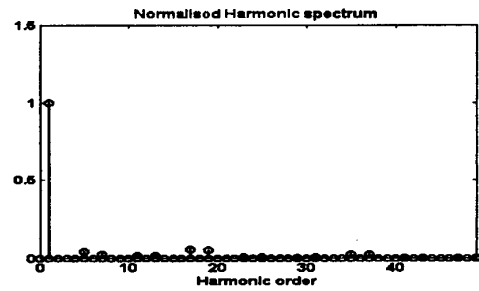


Fig.7d Harmonic spectrum of actual phase voltage (18-step operation)

voltages along a, b, c axes, the modified reference phase voltages after shifting the center 'A' to 'O' are

$$\begin{aligned} V_a(t) &= V_a^*(t) - \frac{2}{9}V_{dc}, V_b(t) = V_b^*(t) + \frac{1}{9}V_{dc}, \\ V_c(t) &= V_c^*(t) + \frac{1}{9}V_{dc} \end{aligned} \quad (7)$$

Using the modified reference phase voltages the inverter switching periods  $T_{ga}$ ,  $T_{gb}$  and  $T_{gc}$  for the mapped sector is calculated and the appropriate inverter output vectors are switched based on the sector selection [4][7].

In a similar way appropriate conditions for all 54 sector selection can be derived and the outer sectors can be mapped to the inner sectors using similar equations as shown in eqn.(7). The details of sector identification, mapping the outer sectors to inner sectors and finally the switching timing and vector selection will be provided in the final paper.

#### IV. Experimental verification

The proposed scheme is simulated for a 1HP open – end winding induction motor drive. The whole system is studied. The drive is operated in V/f mode at various modulation index including the over modulation. Fig.3a and Fig.3b shows the motor phase voltage difference of the pole voltages ( $V_{aa'}$ ) and its triplen harmonic content (Fig.3b) for a modulation index  $V_{dc}=0.2$ . Fig.3c shows the, actual motor phase voltage (triplen content suppressed) and Fig.3d shows the motor phase current under no-load operation for modulation index  $V_{dc}=0.2$ . Since the two inverters are fed from isolated DC power supplies, no triplen harmonic current will flow in the motor phases[3]. Fig.3e shows the triplen voltage content of the phase voltage  $V_{aa'}$  of Fig.3a. Since the two inverters are isolated using transformers (Fig.1), triplen harmonic voltages will not appear across motor terminals (there is no common path for triplen harmonic current and hence no triplen harmonic voltage drop in motor phases). The resultant motor phase voltage without the triplen content is as shown in Fig.3c. The phase voltage envelop is a six-step waveform with low amplitude voltage step changes, when compared to a conventional single 2-level inverter drive. This will result in low amplitude switching harmonic ripples for the proposed scheme, when compared to a conventional scheme. Fig.3f shows the frequency spectrum of the actual motor phase voltage (Fig.3c) for the proposed scheme.

The drive is operated for a modulation index of 0.5 Vdc and the respective waveforms for V/f operation with 0.5 Vdc modulation index are presented in Fig.4. Here the motor phase voltage envelope is a 12- step wave form (fig.4c). Fig.5 shows the various drive waveforms for operation with a modulation index of 0.8 Vdc. Here the motor phase voltage envelope is an 18- step wave form (Fig.5a) Fig.6 and Fig7 shows the waveforms for operation in the over modulation region. Fig.6 shows the drive

waveforms when the drive with PWM traces the outer hexagon and Fig.7 shows the extreme speed range with 18-stepped motor phase voltage.

The salient features of the proposed scheme are

- 6-step, 12-step and 18-step phase voltage waveforms are possible at different speed range.
- As speed increases the phase voltage steps increases and hence switching frequencies can be reduced at higher modulation index for the proposed scheme, when compared to a conventional 2-level single inverter drive. This will result in reduced switching losses and thereby increases the efficiency.
- An 18-stepped wave form is possible at the extreme modulation (over modulation) range as compared six-step in a conventional 2-level inverter drive. This will result in a smooth current waveform with less harmonic content for the proposed drive, in the over modulation region.
- Two 2-level inverters with  $2/3 V_{dc}$  and  $1/3 V_{dc}$  link voltages are needed for the present drive. In the proposed drive configuration the lower voltage inverter is switching more frequent than the high voltage inverter ( $2/3 V_{dc}$  DC link voltage), makes it very suitable for high power drives, with reduced switching losses.
- Isolated DC link voltage control is needed for the present scheme.

#### Appendix

3-phase Induction motor parameters, 400volts, 50 Hz, 4 pole,  $R_1=2.92\text{ohms}$ ,  $R_2=1.61\text{ohms}$ ,  $X_1=X_2= 7.2\text{mH}$ , I no-load=1.5Amps

#### V. References

- [1] A.Nabae, I.Takahashi, and H.Agaki, "A new neutral-point-clamped PWM inverter", IEEE Trans. Ind. Appl. vol. IA-17, pp518-523, Sept./Oct. 1981
- [2] P.M.Bhagwat and V.R.Stefanovic, "Generalized Structure of a multi level PWM inverter", IEEE Trans. Ind. Applicat. vol. IA-19, pp 1057-1069, Nov./Dec. 1983.
- [3] H.Stemmler, P.Guggenbach, "Configurations of high power voltage source inverter drives", EPE.conf- 1993, pp7-12.
- [4] Joohn-Sheok Kim, Seung-Ki Sul, "A Novel Voltage Modulation Technique of the Space Vector PWM", IPEC-1995, pp742-747.
- [5] Bakari Mwinyiwiwa, Zbigniew Wolanski, "Multimodular Multilevel Converters with input/output Linearity", IEEE Trans. Ind. Appl, vol.33, No.5, Sept./Oct. 1997, pp 1214-1219.
- [6] A. Rufer, M. Veenstra, K. Gopakumar, "Asymmetric multilevel converter for high resolution voltage phasor generation", EPE'99-Lausanne, pp. PI-PIO.
- [7] E.G. Shivakumar, K. Gopakumar, S.K. Sinha, Andre Pittet, V.T Ranganathan: "Space vector PWM control of dual inverter fed open-end winding induction drive", IEEE-APEC-2001, pp